Dynamic Jamming Point for Shear Thickening Suspensions

Eric Brown and Heinrich M. Jaeger

The James Franck Institute, University of Chicago, Chicago, Illinois 60637, USA

(Received 3 April 2009; published 20 August 2009)

We report on rheometry measurements to characterize the critical behavior in two model shear thickening suspensions: cornstarch in water and glass spheres in oil. The slope of the shear thickening part of the viscosity curve is found to increase dramatically with packing fraction and diverge at a critical packing fraction ϕ_c. The magnitude of the viscosity and the yield stress are also found to have scalings that diverge at ϕ_c. We observe shear thickening as long as the yield stress is less than the stress at the viscosity maximum. Above this point the suspensions transition to purely shear thinning. Based on these data we present a dynamic jamming phase diagram for suspensions and show that a limiting case of shear thickening corresponds to a jammed state.

DOI: 10.1103/PhysRevLett.103.086001 PACS numbers: 83.80.Hj, 83.60.Rs, 83.85.Cg

In Newtonian fluids the viscosity does not change with an applied shear rate, while non-Newtonian fluids usually show a decrease of viscosity when sheared faster; i.e., they shear thin. The opposite behavior, shear thickening, is less common but can be quite dramatic: beyond a certain shear rate the viscosity increases potentially by orders of magnitude. This behavior is reversible, so the stress relaxes when the shear is removed. Reported shear thickening fluids are usually densely packed colloids or suspensions [1–4], for example, cornstarch in water. Shear thickening is a concern across a range of industrial processes [2,5] and is of interest for the ability to absorb energy from impacts [6].

It has been suggested [4,7–18] that shear thickening is related to the phenomenon of jamming. The concept of a jamming transition, however, applies to the limit of a vanishing shear rate and is exemplified by the onset of glassy behavior with a seemingly diverging viscosity in molecular liquids, dense packings of colloids, or macroscopic granular materials, leading to the appearance of a yield stress below which there is no flow [19–21]. Shear thickening, on the other hand, occurs at nonzero shear rate. While a yield stress has been measured in some shear thickening fluids [9], no link has been established between such yield stress and the observed shear thickening behavior. Some shear thickening fluids have been reported to exhibit seemingly discontinuous jumps in stress with increasing shear rate at high packing fractions, known as discontinuous shear thickening [8,15,18,22–26]. However, this discontinuity has not yet been characterized quantitatively. A model with soft-shell particles found distributions of forces between particles similar to those of force chains in jammed systems [11] but cannot reproduce the dramatic increases in viscosity with shear rate observed in discontinuous shear thickening. As a result, the connection between shear thickening and jamming has not been been made quantitatively.

Here we characterize the stress-shear rate discontinuity and the relationship to the yield stress through rheological measurements. This is the first characterization of discontinuous shear thickening for different packing fractions in non-Brownian suspensions. We find that discontinuous shear thickening is a limiting behavior which is approached at a critical packing fraction where the onset shear rate of shear thickening approaches zero and the yield stress jumps dramatically. In other words, the limiting case of discontinuous shear thickening corresponds to a jammed state. We then develop a phase diagram to delineate the shear thickening and jammed regimes.

We present below experimental results from two rather different hard particle suspensions, cornstarch in water and glass spheres in mineral oil, to demonstrate the generality of our results. Cornstarch (average particle diameter of 14 μm) was chosen as a prototypical shear thickener, while glass spheres (88–125 μm diameter) have the advantages of better defined particle properties and better studied packing properties. The starch particles were suspended in water, density matched to 1.59 g/mL by dissolving CsCl. Using optical tweezers we found no attractions or repulsions outside the range of contact relevant in the stress range of the experiments. Measured starch masses include some water at ambient conditions of 23 °C and 42% humidity. Glass spheres with hydrophobic coating were used to optimize dispersion in mineral oil (viscosity 58 mPa · s) and minimize the yield stress. Packing fractions ϕ are based on measured particle and fluid masses mixed together before shearing.

Measurements were performed in a rheometer using Couette (inner rotating cylinder of diameter 26.6 mm, gap of 1.13 mm) or parallel plate (25 mm diameter rotating top plate) geometries. Care was taken so that no fluid extended outside the parallel plates so the particles were confined to the space between the plates by surface tension. All data presented were taken by controlling the torque T converted to a bulk shear stress τ. The shear rate $\dot{\gamma}$ is defined by the measured rotation velocity over gap size [27]. We define viscosity by $\eta \equiv \tau/\dot{\gamma}$. Samples were presheared before experiments to ensure repeatability. Measurements were performed with increasing as well as

decreasing stress ramps at different ramp rates to check for hysteresis, thixotropy, and transients. We used measurements for different gap sizes to check for finite size effects, and different plate surfaces to check for slip. No differences were found that are significant enough to affect the conclusions presented here. Since glass spheres are denser than mineral oil, measurements were performed in the parallel plate geometry with a gap size of 0.5 mm to minimize possible sedimentation effects. At this gap size we confirmed the results are the same as in a density-matched fluid.

Figure 1 shows stress vs shear rate traces for different packing fractions. On a log-log plot a slope of 1 corresponds to Newtonian flow (indicated by dashed lines for reference), a slope between zero and unity corresponds to shear thinning, while a slope greater than unity signals shear thickening. The overall steepness of the traces within the shear thickening region is seen to increase with ϕ and to approach a vertical line where shear thickening becomes discontinuous. Another feature is that shear thickening occurs over an intermediate stress range that varies little with packing fraction when the yield stress is well below this range. For stresses either larger than the upper limit of the shear thickening region or smaller than the shear thickening onset, shear thinning behavior is observed. At lower ϕ the slopes gradually approach 1 at all stress ranges so there is a gradual transition to Newtonian flow. The behavior described above is similar to what has been found by careful measurements in shear thickening colloids [26]. This is notable because it is usually assumed that Brownian motion and electrostatics are important factors in shear thickening [3]; both are insignificant for our larger particles. At sufficiently large ϕ, the traces exhibit a nonzero stress value in the limit of zero shear rate, i.e., a yield stress. Given a stress resolution around 10^{-2} Pa with our rheometer, this is most clearly seen in the cornstarch data where the yield stress is larger. The yield stress is seen to encroach on the shear thickening stress range at high packing fractions above which there is only shear thinning.

To quantify the stress-strain relationship in the shear thickening region, we fit the traces locally to a power law $\eta \propto \tau^{1-\epsilon}$ which is equivalent to $\tau \propto \dot{\gamma}^{1/\epsilon}$ but it does not diverge so it can be fit more conveniently. The parameter ϵ depends on the packing fraction and corresponds to the inverse slope of the traces in Fig. 1. Newtonian flow corresponds to $\epsilon = 1$, and a stress discontinuity corresponds to $\epsilon = 0$. In Figs. 2(a) and 2(b), the ϵ values plotted are from fits around the steepest portions of the stress-shear rate traces. For both starch particles and glass spheres, ϵ approaches zero at a critical packing fraction ϕ_c where the slope of the viscosity curve becomes divergent. Previous reports have suggested there is a packing fraction above which the stress-shear rate curve becomes discontinuous [26], implying the possibility of $\epsilon = 0$ over a range of ϕ. However, the fact that ϵ only approaches zero at ϕ_c suggests the discontinuity is better thought of as a limiting behavior of shear thickening. The value of ϕ_c is obtained

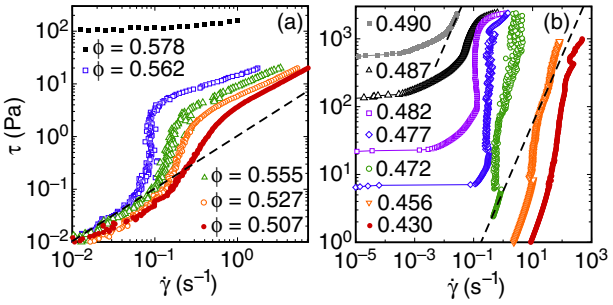

FIG. 1 (color online). Shear stress τ vs shear rate $\dot{\gamma}$ for packing fractions ϕ, as indicated. (a) Glass spheres in mineral oil. (b) Cornstarch in water. Dashed lines: slope 1 indicating fixed viscosity.

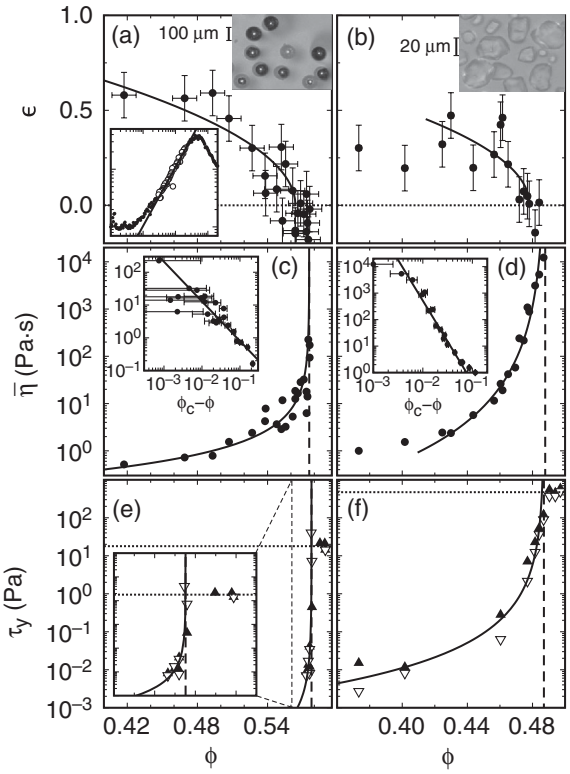

FIG. 2. Evolution of viscosity and yield stress with packing fraction ϕ for glass spheres in mineral oil (a,c,e) and cornstarch in water (b,d,f). (a,b) Inverse logarithmic slope ϵ of stress-shear rate traces in the shear thickening regime, defined by $\tau \propto \dot{\gamma}^{1/\epsilon}$. Lower left inset: an example fit of viscosity vs stress on a log-log scale for $\phi = 0.562$. The open symbols represent the fit range. Upper right insets: micrographs of the particles. (c,d) Viscosity scale $\bar{\eta}$ defined as a geometric mean of the viscosity in the shear thickening region. Insets in (c,d): log-log plots of the same data relative to ϕ_c. (e,f) Yield stress τ_y. Solid triangles: increasing stress measurements. Open triangles: decreasing stress measurements. Dotted lines: the plateau yield stress $\tau_{y,\max}$. Inset in (e): detailed view of the region close to ϕ_c. All panels: Solid lines are power law fits explained in the text; dashed lines are resulting values of ϕ_c.

from a power law fit of $\epsilon \propto (\phi_c - \phi)^n$ to the data in Figs. 2(a) and 2(b) which gives $\phi_c = 0.478 \pm 0.003$ and $n = 0.5 \pm 0.2$ for starch and $\phi_c = 0.564 \pm 0.004$ and $n = 0.5 \pm 0.2$ for glass with relative statistical uncertainties. Power laws shown are fit from ϕ_c down to the smallest ϕ which is consistent with a power law fit. When the lower end of the fit range of ϕ was increased, fit values of ϕ_c remained consistent within quoted uncertainties; however, fit values for exponents varied with the fit range, so we do not claim to have measured limiting scaling exponents with certainty.

As a second indicator of a transition near ϕ_c, we investigate the evolution of the viscosity magnitude. To this end, we define a characteristic magnitude $\bar{\eta}$ by the geometric mean of the viscosity over a fixed stress range in the shear thickening region: for starch in water we use 500 to 1000 Pa, and for glass spheres in mineral oil 0.3 to 1 Pa. Figures 2(c) and 2(d) show that $\bar{\eta}$ appears to diverge very close to the point where ϵ goes to zero. A diverging power law $\bar{\eta} \propto (\phi_c - \phi)^{-n}$ is fit to the data in Figs. 2(c) and 2(d) which gives $\phi_c = 0.488 \pm 0.004$ and $n = 3.1 \pm 0.3$ for starch and $\phi_c = 0.576 \pm 0.004$ and $n = 1.2 \pm 0.2$ for glass. While the viscosity varies with stress, the fit value of ϕ_c is independent of the fixed stress range chosen for the fit in the shear thickening region. This divergent scaling is independent of the yield stress because it is in a much higher stress range, and is independent of the diverging slope because that has a mild effect on a fixed stress range.

The yield stress τ_y for different packing fractions is shown in Figs. 2(e) and 2(f) and is found to increase precipitously as the same value ϕ_c is approached. Around ϕ_c, the yield stress plateaus at a value $\tau_{y,\max}$ and does not change significantly at higher packing fractions. A power law $\tau_y \propto (\phi_c - \phi)^{-n}$ is fit to the data in Figs. 2(e) and 2(f) below the plateau to obtain $\phi_c = 0.487 \pm 0.003$ and $n = 2.5 \pm 0.3$ for starch and $\phi_c = 0.578 \pm 0.004$ for glass spheres (n could not be fit with any certainty because the jump in yield stress is so dramatic). Comparison of the packing fraction dependence of ϵ, $\bar{\eta}$, and τ_y in Fig. 2 shows that, statistically consistent within experimental uncertainties, a single value ϕ_c can represent all three parameters for each of the two suspensions.

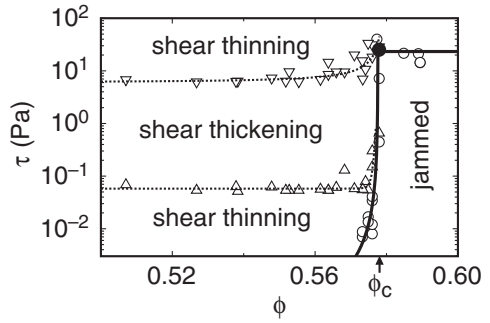

FIG. 3. Dynamic jamming phase diagram for shear thickening fluids. Data shown are for glass spheres in mineral oil. The solid line corresponds to the yield stress in Fig. 2(e), while the dotted lines indicate transitions between shear thinning and thickening. Solid circle: dynamic jamming point at ϕ_c. Open circles: yield stress. Up-pointing triangles: onset of shear thickening. Down-pointing triangles: shear thickening maximum.

From the data in Figs. 1 and 2 we can assemble a phase diagram that delineates shear thinning, shear thickening, and jammed regions in a parameter space given by the applied stress τ_y and the packing fraction ϕ. Figure 3 shows this for the glass spheres. The jammed region here is defined as the portion in the diagram below the yield stress. As in the usual jamming phase diagram [19], exceeding the yield stress leads to shear thinning flow. For $\phi < \phi_c$, a new feature in Fig. 3 are two boundaries that extend out from the jammed region to smaller packing fractions. These boundaries separate shear thickening from shear thinning regimes. Increasing stress at fixed ϕ will take a sample from shear thinning to thickening and back to thinning again, as seen from the slope changes of $\tau(\dot{\gamma})$ in Fig. 1. As ϕ_c is approached from below, however, the increasing yield stress pushes both boundaries upward, forcing them to approach the yield stress line that delineates the jammed region. Once the yield stress dominates the total stress in the system, the suspension no longer exhibits shear thickening behavior but only jamming and shear thinning. Because of the divergent scaling of the yield stress, this transition occurs at a packing fraction near to but less than ϕ_c. Since the onset stress for shear thickening (up-pointing triangles in Fig. 3) lies above the yield line, the shear thickening and jamming regions are separated by a thin wedge of shear thinning. The convergence of the yield stress and the boundaries between shear thickening and shear thinning suggests that ϕ_c is a singular point. We name this the *dynamic jamming point* because it is analogous to a static jammed state with a yield stress in the sense that the slope divergence at ϕ_c implies the stress increases without an increase in shear rate, i.e., exhibits a jump in $\tau(\dot{\gamma})$. Furthermore, since the viscosity magnitude diverges in $\phi_c - \phi$ and the onset shear stress of the shear thickening regime is relatively fixed (except for the influence of the yield stress), the shear rate required for shear thickening extrapolates to zero at ϕ_c. Thus, the discontinuous shear thickening limit corresponds to a jammed state. We note, however, that the approach to zero onset shear rate cannot be measured all the way up to ϕ_c because the diverging yield stress suppresses shear thickening before ϕ_c is actually reached. This extrapolation is made without reference to the yield stress measurements; the observation that this dynamic jamming point occurs on the jamming phase boundary confirms the correspondence.

While details differ for cornstarch and glass spheres, both show qualitatively similar behavior in terms of divergences and the delineation of jammed, shear thickening and shear thinning regions in Fig. 3. The fact that we observe this for very different suspensions and measuring methods suggests this behavior is robust for suspensions of nonattractive particles. Attractive particles usually do not

shear thicken [2] and can have a jamming point at much lower packing fractions [28]. We found the boundary condition to be important as suggested by [13,18]. In the parallel plate setup, when the experiment was done instead with extra fluid extending outside the plates, the shear thickening traces were less steep, and a divergent scaling of the slope was not achieved. This suggests that confinement (in this case by surface tension) is necessary to observe the discontinuous shear thickening limit.

Finally, we turn to the significance of the measured value for ϕ_c. Given uncertainty on the order of 0.1 in determining an absolute packing fraction for starch samples due to water absorption from the atmosphere and the internal structure of the starch particles, and given less knowledge of packing properties of polydisperse powders [Fig. 2(b) inset], we focus instead on the glass spheres. Their packing fraction is well defined, and their packing properties are well studied. We find near identical values for ϕ_c when the fluid is replaced by silicone oil or water, or when we double the particle size. Thus ϕ_c is not determined by fluid properties or particle diameter but rather is an issue of geometric packing. For glass spheres, we have an average value of $\phi_c = 0.573 \pm 0.013$ including an absolute error of 0.005. This packing fraction is consistent with $\phi = 0.57$ for mechanically stable packings found by slowly settling glass spheres with the same density mismatch in our experiment [29–31]. In the limit of zero mismatch this would correspond to random loose packing $\phi_{\mathrm{rlp}} = 0.56$ [29,30]. Without friction or gravity this would correspond to random close packing $\phi_{\mathrm{rcp}} = 0.64$ [21]. If a mechanically stable packing exists, it must have a yield normal stress holding itself up against gravity on the order of $\Delta\rho g d \approx 10$ Pa for a layer $d = 0.5$ mm thick. Supposing that the value of the yield stress is on the same order of magnitude for normal and shear directions, we expect that the jamming point occurs when the yield stress crosses this threshold, which is seen in Fig. 3 in the approach as $\phi \rightarrow \phi_c$. This agreement confirms that ϕ_c corresponds to the jamming point.

The existence of divergent scalings at a critical packing fraction is provocatively reminiscent of a 2nd order phase transition. While the jamming point has been shown to have similarities to a critical point with some nonuniversal critical exponents [21], and some scalings compatible with a 2nd order phase transition [32], we are not aware of any such model that includes shear thickening.

We thank T. Witten and S. Nagel for thoughtful discussions, and Jing Xu for help with the optical tweezer measurements. This work was supported by DARPA through Army Grant No. W911NF-08-1-0209 and by the NSF MRSEC program under DMR-0820054.

[1] J. F. Brady and G. Bossis, Annu. Rev. Fluid Mech. **20**, 111 (1988).
[2] H. A. Barnes, J. Rheol. **33**, 329 (1989).
[3] B. J. Maranzano and N. J. Wagner, J. Chem. Phys. **114**, 10 514 (2001).
[4] P. Hébraud and D. Lootens, Mod. Phys. Lett. B **19**, 613 (2005).
[5] D. Lootens, P. Hébraud, E. Lécolier, and H. Van Damme, Oil Gas Sci. Technol. **59**, 31 (2004).
[6] Y. S. Lee, E. D. Wetzel, and N. J. Wagner, J. Mater. Sci. **38**, 2825 (2003).
[7] M. E. Cates, J. P. Wittmer, J.-P. Bouchaud, and P. Claudin, Phys. Rev. Lett. **81**, 1841 (1998).
[8] E. Bertrand, J. Bibette, and Véronique Schmitt, Phys. Rev. E **66**, 060401(R) (2002).
[9] D. Lootens, H. Van Damme, and P. Hébraud, Phys. Rev. Lett. **90**, 178301 (2003).
[10] C. B. Holmes, M. Fuchs, and M. E. Cates, Europhys. Lett. **63**, 240 (2003).
[11] J. R. Melrose and R. C. Ball, J. Rheol. **48**, 961 (2004).
[12] C. B. Holmes, M. E. Cates, M. Fuchs, and P. Sollich, J. Rheol. **49**, 237 (2005).
[13] M. E. Cates, M. D. Haw, and C. B. Holmes, J. Phys. Condens. Matter **17**, S2517 (2005).
[14] J. Delhommelle and J. Petravic, J. Chem. Phys. **123**, 074 707 (2005).
[15] D. Lootens, H. van Damme, Y. Hémar, and P. Hébraud, Phys. Rev. Lett. **95**, 268302 (2005).
[16] M. Sellitto and J. Kurchan, Phys. Rev. Lett. **95**, 236001 (2005).
[17] F. D. Ianni, D. Lasne, R. Sarcia, and P. Hébraud, Phys. Rev. E **74**, 011401 (2006).
[18] A. Fall, N. Huang, F. Bertrand, G. Ovarlez, and D. Bonn, Phys. Rev. Lett. **100**, 018301 (2008).
[19] A. Liu and S. Nagel, Nature (London) **396**, 21 (1998).
[20] A. J. Liu and S. R. Nagel, *Jamming and Rheology: Constrained Dynamics on Microscopic and Macroscopic Scales* (Taylor and Francis, London, 2001).
[21] C. S. O'Hern, L. E. Silbert, A. J. Liu, and S. R. Nagel, Phys. Rev. E **68**, 011306 (2003).
[22] R. L. Hoffmann, Trans. Soc. Rheol. **16**, 155 (1972); J. Colloid Interface Sci. **46**, 491 (1974); Adv. Colloid Interface Sci. **17**, 161 (1982).
[23] H. M. Laun, J. Non-Newtonian Fluid Mech. **54**, 87 (1994).
[24] W. J. Frith, P. d'Haene, and R. Buscall, J. Rheol. **40**, 531 (1996).
[25] J. Bender and N. Wagner, J. Rheol. **40**, 899 (1996).
[26] R. G. Egres and N. J. Wagner, J. Rheol. **49**, 719 (2005).
[27] These conversions to shear stress and rate are standard in rheometry and characterize the depth averaged mechanical response in a geometry-independent form. We do not imply a constant local shear rate, i.e., a Newtonian velocity profile.
[28] V. Trappe, V. Prasad, L. Cipelletti, P. N. Segre, and D. A. Weitz, Nature (London) **411**, 772 (2001).
[29] G. Y. Onoda and E. G. Liniger, Phys. Rev. Lett. **64**, 2727 (1990).
[30] M. Jerkins, M. Schröter, H. L. Swinney, T. J. Senden, M. Saadatfar, and T. Aste, Phys. Rev. Lett. **101**, 018301 (2008).
[31] A slight negative correction might be expected because of the finite sample size [30]; however, since we see no effect of changing the gap size, this correction is unnecessary.
[32] P. Olsson and S. Teitel, Phys. Rev. Lett. **99**, 178001 (2007).